

Uplift resistance of buried submarine pipelines: comparison between centrifuge modelling and full-scale tests

A. C. PALMER*, D. J. WHITE*, A. J. BAUMGARD*, M. D. BOLTON*, A. J. BAREFOOT*, M. FINCH†, T. POWELL†, A. S. FARANSKI* and J. A. S. BALDRY*

A buried pipeline can buckle upwards if there is not enough resistance to movement. Both the uplift resistance (the maximum force per unit length) and the mobilisation distance (the distance the pipeline has moved before the maximum force is reached) are important in design. Tests on pipes in several soils were carried out at 1 g at full scale and in a centrifuge at 10 g and 1/10 scale. A comparison shows that the measured uplift resistances are consistent with the conventional understanding of centrifuge tests, but that the measured mobilisation distances are not consistent with that understanding. Unscaled mobilisation distance in the centrifuge is roughly the same as at full scale. Mobilisation distance does not scale with particle size. This discrepancy is related to the formation of shear zones, and to theory and observations in other areas of the mechanics of brittle materials, among them ice, concrete and heavily overconsolidated clays. An idealised analytical model displays the same behaviour.

KEYWORDS: buried structures; centrifuge modelling; deformation; offshore engineering; solid/structure interaction; trenches

Un pipeline enfoui peut se redresser en se courbant s'il ne rencontre pas assez de résistance à ce mouvement. La résistance au redressement (la force maximum par longueur unitaire) et la distance de mobilisation (la distance accomplie par le pipeline avant que la force maximum ne soit atteinte) sont deux critères importants lors de la conception. Des essais sur des pipelines installés dans plusieurs sols ont été réalisés avec 1 g et dans une échelle grandeur nature ainsi que dans une centrifugeuse avec 10 g et une échelle d'un dixième. Une comparaison montre que les résistances au redressement mesurées correspondent bien aux interprétations conventionnelles des essais centrifuges mais que les distances de mobilisation mesurées ne correspondent pas à cette interprétation. La distance de mobilisation, sans mise à échelle, dans la centrifugeuse est en gros la même que celle à grande échelle. La distance de mobilisation n'est pas proportionnelle à la dimension des particules. Cette différence est liée à la formation de zones de cisaillement et à la théorie et aux observations en mécanique des matières friables comme la glace, le béton et les argiles extrêmement surconsolidées. Un modèle analytique idéal montre le même comportement.

INTRODUCTION AND BACKGROUND

Centrifuge modelling has become a widely used technique in geotechnical engineering. Opportunities to make direct comparisons between full-scale prototype behaviour and model behaviour in the centrifuge have been infrequent, because most prototype geotechnical constructions are physically large, so that field tests are expensive, and also because natural soils have a complex fabric and spatial variability that is not easy to represent in a scaled model. Opinions about the way centrifuge modelling should be used in geotechnical practice have been varied and controversial. One argument has been that models are not meant to be literal representations of a prototype, but that they are most powerfully used to throw light on mechanisms, which once understood can be further analysed by different techniques such as finite element analysis.

A good opportunity to make a comparison between model and full-scale behaviour arose from research into upheaval buckling of buried pipelines. A constrained pipeline buckles when the longitudinal compressive force induced by the operating temperature and pressure interacts with a 'hill' in the pipeline profile, called an *overbend* in the jargon of pipeline practice. The interaction between the compressive force and the curvature tends to make the pipeline push upwards at the crest of the overbend. The pipeline's own

weight, and the uplift resistance of the soil it is buried in, help to hold the pipeline down. If the weight and uplift resistance are not large enough to hold the pipeline in place, it moves upwards. Once it starts to move, the curvature increases locally, and the uplift resistance generally decreases, and so the pipeline becomes unstable and jumps to a new equilibrium position, often some way above ground level. The movements can be sudden and dramatic: Aynbinder & Kamershtein (1982) cite an example of a 1020 mm (40 in) pipeline that moved out of the ground over a distance of some 70 m, to a new equilibrium with the pipe axis 4.2 m above the surface. The theory and a case study are described in a number of papers (Palmer & Baldry, 1974; Nielsen *et al.*, 1990; Palmer *et al.*, 1990; Palmer *et al.*, 1994).

Upheaval can be prevented by making sure that the cover material is heavy and deep enough to provide the necessary uplift resistance. Marine pipelines are protected against upheaval either by dumping rock over them or by trenching them with a plough and then backfilling the ploughed-out natural seabed material over the pipeline. Both operations are expensive, and it is important to understand both how much uplift resistance a given cover depth secures, and how far the pipeline will move before the resistance is mobilised.

EXPERIMENTAL PROGRAMME

Unusually for a problem in geotechnics, the scale of the prototype is relatively small. This made it possible to carry out laboratory experiments at nearly full scale in the Schofield Centre of Cambridge University Engineering Department. Baumgard (2000) describes the experimental details, and Fisher *et al.* (2002) present some of the results in a

Manuscript received 8 May 2003; revised manuscript accepted 16 September 2003.

Discussion on this paper closes 1 June 2004, for further details see p. ii.

* Cambridge University Engineering Department, Cambridge, UK.

† Coflexip Stena Offshore Ltd, Aberdeen UK.

paper directed towards pipeline engineers. The experiments were carried out for Coflexip Stena Offshore Limited (CSO), now Technip-Coflexip, a pipeline construction contractor.

The apparatus was straightforward, and comprised a 220 mm diameter PVC pipe 1150 mm long buried in saturated soil in a tank, a system of lead screws to move the pipe vertically under displacement control, load cells to measure the uplift resistance, and transducers to measure the displacement. The soils tested were rock, dense sand, fine sand and a fine cohesionless silt; their properties are summarised in Table 1. Loose silt and sand fills were prepared by filling the tank with water and raining the soil through a 2 mm sieve just below the water surface. Dense sand fills were prepared by placing 100 mm lifts, raising the water level above the sand surface, and then vibrating with a poker applied in a grid pattern. The same process could not be used for dense silt fills, because the poker left holes, and instead the dense fills were prepared from preconsolidated 50–100 mm blocks. Rock fills were prepared by tipping and then flooding.

A parallel programme of 1/10-scale centrifuge experiments at 10g was carried out in the Cambridge mini-drum centrifuge, described fully by Barker (1998). The apparatus and experimental methodology used for these experiments are described by Barefoot (1997) and White *et al.* (2000). The model pipe was 22 mm in diameter and 120 mm long. The soil was Fraction D silica sand supplied by David Ball Limited. Its maximum and minimum voids ratios are 0.98 and 0.69, and the relative density (relative voids ratio), I_D , was 44% in all three tests. The critical state angle of friction in a shear box is 32°.

EXPERIMENTAL RESULTS

Figure 1 plots force per unit length during an uplift test against upward displacement for two full-scale tests at 1g, one in dense sand and one in loose sand. Fig. 2 is the same plot for 10g centrifuge tests M1 to M3. The displacements are those measured: they have not been scaled.

Figure 3 compares the 1g and 10g tests by plotting a non-dimensional uplift resistance against a non-dimensional displacement. The non-dimensional uplift resistance, F^* , is defined by

$$F^* = \frac{F}{\gamma DH} \tag{1}$$

where F is the force per unit length of pipe, γ is the unit weight of the soil above the pipe (submerged unit weight if the soil is under water and saturated), D is the pipe outside diameter, and H is the initial cover (measured from the top of the pipe to the soil surface).

The non-dimensional displacement is the displacement, U , of the pipe, divided by D .

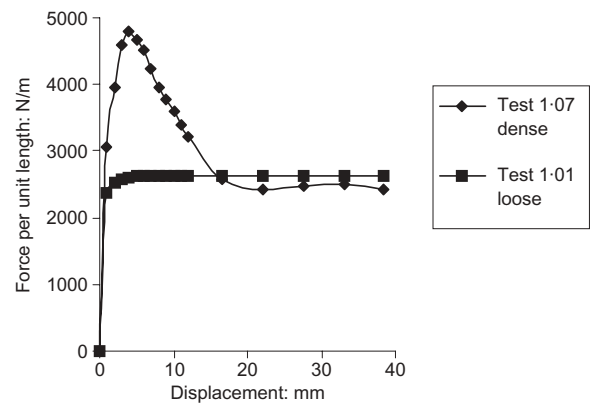


Fig. 1. Relation between displacement and force in 1g tests on 220 mm pipe

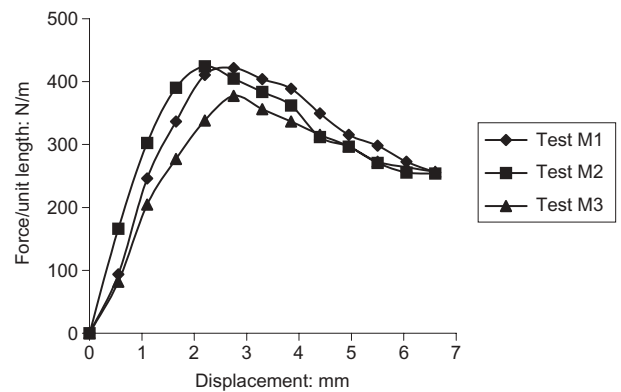


Fig. 2. Relation between displacement and force in 10g tests on 22 mm pipe

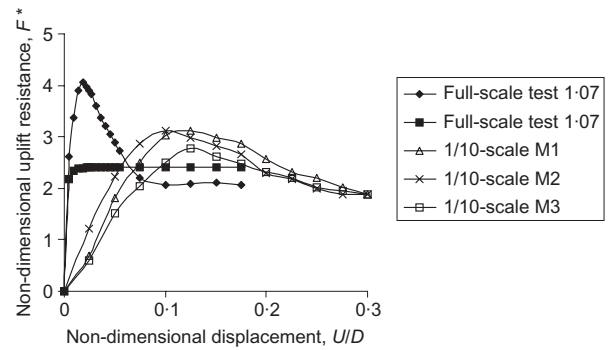


Fig. 3. Relation between non-dimensionalised displacement and non-dimensionalised force, F^* . Solid symbols represent full-scale tests; open symbols represent 10g centrifuge tests

Table 1. Soil properties

| Material | Limestone silt | Fraction D fine sand | Fine-medium sand | Flint rockdump | Sandy clayey silt |
|--------------------------------------|----------------|----------------------|------------------|----------------|-------------------|
| D_{10} : mm | 0.022 | 0.20 | 0.25 | 20 | |
| D_{50} : mm | 0.031 | 0.27 | 0.42 | 50 | |
| D_{90} : mm | 0.11 | 0.32 | 2.0 | 110 | |
| e_{max} | 1.05 | 1.06 | na | na | na |
| e_{min} | 0.66 | 0.61 | na | na | na |
| Angle of friction, ϕ' : degrees | 25.5 | 32 | na | 38 | 36 |
| Particle specific gravity | 2.69 | 2.65 | 2.65 | 2.65 | 2.52 |
| LL: % | | | | | 70 |
| PL: % | | | | | 30 |

DISCUSSION

Figure 3 shows that the centrifuge test matches the results of the 1g tests well. The relationship between F^* and the cover to diameter ratio, H/D , is often taken to be

$$F^* = 1 + \frac{fH}{D} \quad (2)$$

where f is an uplift resistance coefficient, determined by experiment and for sand generally found to be between 0.5 and 1. Recalling that H/D is 3.14 for the centrifuge tests and 2.63 for the 1g tests, the results are consistent with values in that range.

The displacements are predicted much less well. A comparison between Fig. 1 and Fig. 2 shows that the displacement to the peak load is about 4 mm at full-scale and between 2 mm and 3 mm in the 10g centrifuge test, so that the displacements to peak are nearly the same in both cases.

Centrifuge modelling applies an acceleration field that scales up gravity by the same factor, λ , as lengths are scaled down. Stresses ought then to be the same in the model as at corresponding points in the prototype. If strain is a function only of stress, strains ought to be the same. Displacements scale in the same way as other lengths, and displacements in the prototype ought to be λ times displacements observed in the centrifuge model. Accordingly, if the displacement to peak load is 2.5 mm in a 1/10 scale model tested at 10g, the corresponding displacement in a full-scale prototype ought to be $10 \times 2.5 = 25$ mm. That is plainly not the case in this instance.

The same discrepancy is seen in a plot in terms of non-dimensional parameters in Fig. 3. The mobilisation displacement is a much larger fraction of the pipe diameter in the centrifuge than it is for the prototype. The centrifuge results parallel those of Ng & Springman (1994), who found the ratio of displacement to diameter at peak uplift resistance to be between 0.08 and 0.18.

There is clearly a problem here. The discrepancy in scaling is not just a matter of a small percentage, which might be explained in many ways. Indeed, a model that fits this dataset better is that mobilisation distance does not scale at all, and that it is the same in a centrifuge model as at full scale.

A possibility is that mobilisation displacement scales with particle diameter. Fig. 4 plots mobilisation displacement against D_{50} , both on logarithmic scales, for all the tests in the series carried out for CSO. Because of the difficulty of identifying the precise displacement at the peak, mobilisation displacement is here defined as the displacement at which the uplift resistance first reaches 95% of its maximum value. It is not clear why the mobilisation distances at the largest and smallest particle sizes show much more scatter than those at intermediate sizes, and that may be fortuitous. However, the figure shows that increasing particle diameter by a factor of more than 1000 increases mobilisation displacement by a factor of at most 10. The hypothesis that mobilisation displacement scales with particle diameter is not correct.

A tentative alternative explanation of this phenomenon is that it is associated with the formation and propagation of shear zones. Baldry (1973) carried out pullout tests on a rectangular 25.4 by 3.18 mm bar buried in dry Leighton Buzzard sand ($D_{50} = 0.8$ mm), and made X-ray photographs looking in the direction of the long axis of the bar. Dilatation shows up on the X-rays as lighter areas, because it reduces the density. Fig. 5 shows clearly the initiation and growth of a dilated shear zone that starts at the edges of the bar and propagates upwards toward the surface. Strain localisation in shear zones is an important area of current research: see, for example, Mokni & Desrues (1998) and Roger *et al.* (1998).

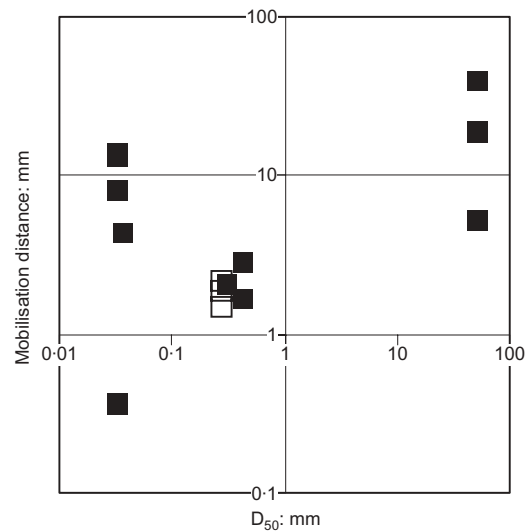


Fig. 4. Relation between particle size (D_{50}) and mobilisation distance. Solid symbols represent full-scale tests; open symbols represent 10g centrifuge tests.

Parallel research on shear zones pursues the link between shear zones in geotechnics and cracks in metals and composites. Palmer & Rice (1973) showed that if a shear zone can be characterised by a relationship between the relative shear displacement and the shear traction, then there are scale effects (Sture *et al.*, 1999), and those effects influence the interpretation of centrifuge tests. Another phenomenon that can be explained in this way is the observation that the relationship between shear displacement in a shear box and shear force per unit shear area is strongly influenced by the length of the shear box (Petley, 1966; Cuckson, 1977). Shorter shear boxes give higher peak strengths, which are reached at smaller displacements (Garnier, 2002).

Similar effects are recognised in several other areas of mechanics. Van Mier (1997, 2001) carried out compression tests on prismatic concrete cylinders of different lengths, and observed that the stress-strain relation is strongly length-dependent. Up to the maximum stress, the strain averaged over the specimen is a function of stress. Beyond the maximum, the nominal strain depends on the length, but there is a unique relationship between stress and displacement of the end platens. Scale effects in ice mechanics (Sanderson, 1988; Palmer & Sanderson, 1991; Palmer & Johnston, 2001) are well known, and are attributed to fracture and the formation of localised 'hot spot' high-pressure zones (Dempsey *et al.*, 2001). Centrifuge test results must scale in a different way in a brittle material characterised by a fracture toughness rather than a yield stress (Palmer, 1991).

In this instance, we consider first a semi-quantitative descriptive explanation and then a more detailed quantitative analysis.

DESCRIPTIVE EXPLANATION

To investigate a possible scale effect on mobilisation distance, we shall model the failure mechanism represented by localisation and shear banding on planes extending from the pipe shoulders towards the ground surface. Localisation is supposed already to have begun, and we are not considering the initial stage of pipe uplift, in which strain is still continuously distributed in the soil above the pipe. The constitutive behaviour can be described by linking shear stress transmitted across the zone to relative displacement across the shear zone.

Suppose that there is a relationship between the relative displacement across a shear zone and the shear stress (shear

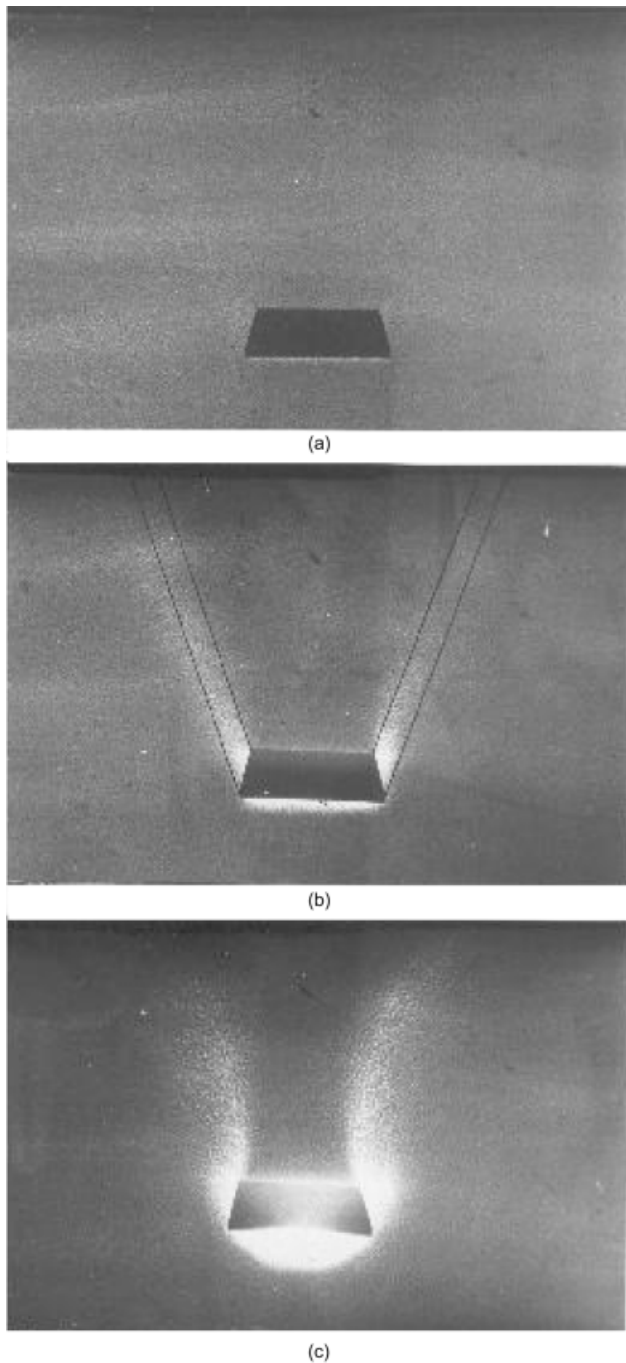


Fig. 5. X-ray photographs looking along axis of lifted bar: (a) $U/D = 0.02$; (b) $U/D = 0.08$; (c) $U/D = 0.30$. U is upward displacement of bar; D is breadth of bar

force/unit area) transmitted across the zone, and that that relationship has the general form shown in Fig. 6(a). At full scale, the mean vertical stress at the level of the top of the pipe is F/D , and it falls to zero over the cover height, H . If the stress falls linearly with distance, and if the ratio between vertical stress and vertical strain is denoted by R , then the relative displacement between the top of the pipe and the soil at the surface is $FH/2RD$. R is simply a ratio between stress and strain; it is not necessarily to be interpreted as an elastic modulus. In a centrifuge test at ng (n times the gravitational acceleration), the stress F/D is the same and R is the same, but the scaled cover height is H/n , and so the relative displacement is $FH/2nRD$. The relative

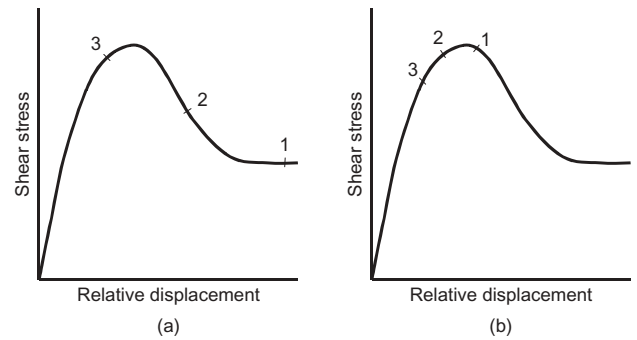


Fig. 6. Relation between shear force and relative displacement across a shear zone: schematic: (a) full scale; (b) centrifuge

displacement scales with n , like other lengths in the centrifuge, and is always smaller in the centrifuge than it is at full scale.

Now consider the interaction between a range of relative displacements and the relationship in Fig. 6. Fig. 6(a) represents full scale and Fig. 6(b) the centrifuge. Points 1, 2 and 3 represent different levels above the pipe, at the same stage of deformation. The relative movement is largest at 1, which is closest to the pipe, and smallest at 3, which is higher up. At full scale, deformation of the soil between points 1, 2 and 3 allows large relative movements, so that the corresponding points are widely spaced. In the centrifuge, the relative movements are much smaller (even though the stress is the same), and corresponding points are much closer together. At each stage of the development of uplift movement, the points in Fig. 6(b) that represent relative displacement will be closer together in the centrifuge than at full scale. In the centrifuge, there will be a stage at which all the relative displacements are close to the peak, whereas at full scale some will be some way past the peak and at the same time some will still be some way before the peak. At full scale, the effect of the peak tends to be smeared out.

In the extreme case when R is large, the relative displacements within the region between the shear zones are always small by comparison with the relative displacement across the shear zones. The pipe displacement at which the uplift resistance reaches a maximum ought then to be the same in the centrifuge as at full scale. That is close to what is observed.

The above description could equally be applied to test on shear boxes of different lengths, L . An increase in L leads to an increased relative displacement along the evolving shear plane. This causes a smearing of the measured peak resistance as different parts of the shear band mobilise peak strength at different stages of the test. This descriptive model predicts that tests in longer shear boxes (higher L) will give lower peak strengths, as is observed (Garnier, 2002).

QUANTITATIVE ANALYSIS

These effects are displayed by the idealised and heavily simplified model depicted in Fig. 7(a). Two shear zones initiate from the points A and B and propagate upwards, and reach the surface at C and D. The regions between AB and the pipe do not deform, but move with the pipe. The soil to the left of AC and to the right of BD does not deform at all. Z is distance measured vertically downward from the soil surface, H is cover in the initial undeformed state, and D is pipe diameter.

Figure 7(b) shows a horizontal slice across the region

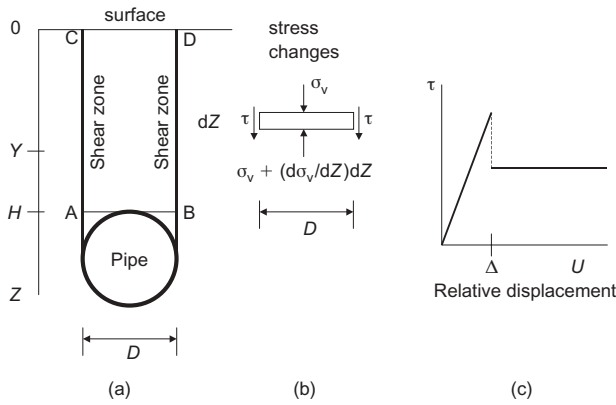


Fig. 7. Idealisation with two vertical shear zones: (a) definition sketch; (b) changes of stress on boundaries of an element of soil between the shear zones; (c) relation between shear stress, ν , and relative displacement, U

between the shear zones. Initially the vertical stress in the soil is uniform horizontally, and at each level balances the weight of the soil above it. The pipe then moves upward, and its movement induces a shear stress, τ , across each shear zone and a change, σ_v (compressive positive), in the mean vertical stress, averaged across the horizontal distance D between AC and BD. From equilibrium:

$$\frac{d\sigma_v}{dZ} = \frac{2\tau}{D} \tag{3}$$

This equation does not include the weight of the soil between the shear zones, because that weight is of course present both before and after the change occurs. Vertical displacement is denoted by U (positive upward). The ratio between the change in σ_v and the change in compressive strain, dU/dZ , is R .

$$\sigma_v = R \frac{dU}{dZ} \tag{4}$$

Once again R is a ratio between change of stress and change of strain: it is not necessarily to be interpreted as an elastic modulus. Combining equations (3) and (4):

$$R \frac{d^2U}{dZ^2} = \frac{2\tau}{D} \tag{5}$$

The relationship between relative displacement across the shear zone and the shear stress is shown in Fig. 7(c), and is taken to be

$$\tau = \begin{cases} \frac{mU}{\Delta} \gamma \mu K Z & \text{if } U < \Delta \\ \gamma \mu K Z & \text{if } U > \Delta \end{cases} \tag{6}$$

where Δ is a mobilisation distance at which the shear stress falls to its value for large relative displacements, m is the ratio between the peak and large-displacement values of τ , γ is the unit weight of the soil (submerged if it is under water), μ is a constant ratio between the shear stress and normal stress across a shear zone, and K is a constant ratio between the horizontal normal stress across a vertical shear zone and the vertical stress at the same level in the initial undisturbed condition.

Equation (6) reflects the expectation that the level of shear stress that can be transmitted across a shear zone will increase with depth, Z , from the surface, in parallel with the mean level of vertical stress before the movement began, and the condition that the shear stress across a vertical shear zone be equal to zero at the surface, since that is required

by local equilibrium. The effect of shear across the zones is to make the vertical stress more compressive between the zones and less compressive outside them. K is not meant to be the conventional K_0 .

This is of course not the only possible idealisation of the relation between shear stress and relative displacement. The key feature is the incorporation of a mobilisation distance, Δ . The idealised model is deliberately simplified, but it is recognised that a complete analysis of uplift involves many complex factors, including inelastic deformation outside the shear zones.

The soil between the shear zones is compressed by the effect of the shear stress, τ , on the vertical stress in the region between the shear zones. It follows that the relative displacement decreases with increasing height above the pipe. The system's response to upward movement of the pipe can be divided into three phases. In the first phase, the displacement, U , is less than Δ everywhere between the pipe and the surface. In the second phase, the displacement is greater than Δ at the pipe and over the lower part of the region between the shear zones, but less than Δ over the upper part of the region; the displacement reaches Δ at a distance Y below the surface. In the third phase, the displacements are greater than Δ throughout the region above the pipe.

Consider first the region in which $U < \Delta$. Combining equation (5) and the first of equation (6):

$$\frac{d^2U}{dZ^2} = \left(\frac{2m\gamma\mu K}{RD\Delta} \right) UZ \tag{7}$$

It is helpful to non-dimensionalise all length variables with respect to a characteristic length λ , defined as

$$\lambda = \left(\frac{ERD\Delta}{2m\gamma\mu K} \right)^{1/3} \tag{8}$$

and to denote the dimensionless variables by lower case symbols, so that

$$\begin{aligned} z &= Z/\lambda \\ u &= U/\lambda \\ h &= H/\lambda \\ y &= Y/\lambda \end{aligned} \tag{9}$$

Equation (7) then has the simple form

$$\frac{d^2u}{dz^2} = uz \tag{10}$$

whose general solution is

$$u = c_1 Ai(z) + c_2 Bi(z) \tag{11}$$

where c_1 and c_2 are integration constants and Ai and Bi are the Airy functions (Abramowitz & Stegun, 1964).

In the region in which $U > \Delta$, combining equation (7) and the second of equation (6) and applying the same non-dimensionalisation:

$$\frac{d^2u}{dz^2} = \frac{\Delta}{\lambda m} z \tag{12}$$

which can be integrated directly to the general solution

$$u = \frac{\Delta}{\lambda m} \frac{z^3}{6} + c_3 z + c_4 \tag{13}$$

The integration constants c_1 to c_4 in equations (11) and (13) are straightforwardly determined by applying the boundary conditions. The derivative du/dz is zero at the surface $z = 0$ because σ_v must remain zero there. In phase 2, u is Δ/λ at $z = y$ and du/dz is continuous at $z = y$ (because σ_v must be continuous). The solutions are:

- (a) in phase 1, when $U(h)$, the displacement at the top of the pipe, is less than Δ :

$$u = \frac{U(h)}{\lambda} \frac{\sqrt{3}Ai(z) + Bi(z)}{\sqrt{3}Ai(h) + Bi(h)} \quad (14)$$

- (b) in phase 2, when $U(h) > \Delta$ but the displacement at the surface, $U(0)$, has not reached Δ :

$$u = \frac{\Delta}{\lambda} + \frac{\Delta}{2\lambda m} \left(\frac{1}{3}z^3 - zy^2 + \frac{2}{3}y^3 \right) + (z-y) \frac{\Delta}{\lambda} \frac{\sqrt{3}Ai'(y) + Bi'(y)}{\sqrt{3}Ai(y) + Bi(y)} \quad \text{in } z > y \quad (15)$$

$$u = \frac{\Delta}{\lambda} \frac{\sqrt{3}Ai(z) + Bi(z)}{\sqrt{3}Ai(y) + Bi(y)} \quad \text{in } z \leq y$$

- (c) in phase 3, when $U(0) > \Delta$:

$$u = \frac{U(h)}{\lambda} + \frac{1}{6} \frac{\Delta}{\lambda m} (z^3 - h^3) \quad (16)$$

where primes denote differentiation. The origin of the $\sqrt{3}$ is the fact that $Ai'(0) = -Bi'(0)/\sqrt{3}$. The change of vertical stress can be determined from equation (4) and du/dz . The additional vertical force per unit length is the change of vertical stress at the top of the pipe multiplied by the pipe diameter, D .

These results allow numerical experiments akin to 'modelling of models' in the centrifuge. The following values are representative of an underwater buried pipeline that might suffer from upheaval buckling:

| | |
|----------|-------------------------|
| D | 0.273 m (nominal 10 in) |
| H | 1 m |
| Δ | 0.005 m |
| m | 1.5 |
| R | 10^6 N/m ² |
| γ | 10 kN/m ³ |
| μ | 0.5 |
| K | 0.6. |

Figure 8 plots the non-dimensional uplift resistance, F^* , calculated from the above model against $U(h)/D$, the ratio between displacement at the pipe and diameter. The maximum value of F^* is 2.23, which is reached when U/D is 0.029.

A 10g centrifuge model can be simulated by dividing the lengths D and H by 10, multiplying the unit weight γ by 10, and letting the other parameters maintain the same values. Fig. 8 also plots F^* against U/D for that case. The

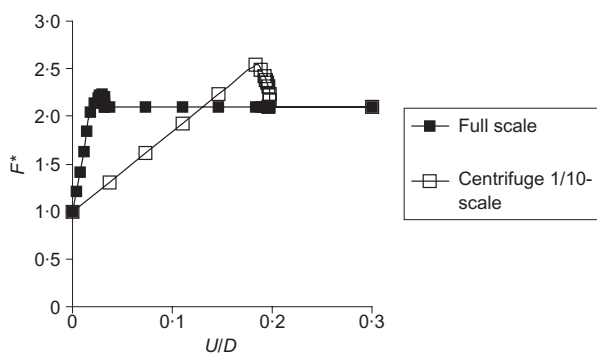


Fig. 8. Relation between non-dimensionalised displacement, U/D , and non-dimensionalised force, F^* , derived from idealisation in Fig. 7. Solid symbols represent full scale; open symbols represent 10g in the centrifuge

maximum value of F^* is 2.55, which is reached when U/D is 0.183.

A comparison between Fig. 8 and Fig. 3 shows that the model exhibits some of the discrepancies between the full-scale and centrifuge-scale tests. The peak value of F^* is slightly higher in the centrifuge model, and the normalised displacement to peak F^* is considerably higher. The model demonstrates that only part of the mobilisation displacement scales in accordance with the conventional understanding of centrifuge tests.

CONCLUSIONS

A comparison between uplift resistance tests on a prototype pipe at 1g and a 1/10-scale model at 10g indicates that the observed displacements are in that instance not consistent with the accepted understanding of centrifuge tests. This discrepancy can tentatively be explained as an effect of localised shear zones across which the shear stress is a function of the relative displacement, and a simple model is consistent with that.

ACKNOWLEDGEMENTS

Most of this work was carried out under a research contract between Coflexip Stena Offshore Limited (CSO) and Cambridge University, and the authors are grateful to CSO for permission to publish it. It is related to parallel work on the fracture mechanics of ice within the LOLEIF Project in the framework of the EU-sponsored Marine Science and Technology (Mast-III) Programme under contract no. MAS3-CT97-0078 and the current STRICE project under contract no. EVG 1-CT-2000-00024. Andrew Palmer's research is supported by the Jafar Foundation, and this paper was written during a sabbatical year at Harvard University. Amy Faranski's research was in part supported by the Churchill Foundation.

The authors thank several reviewers for their comments.

REFERENCES

- Abramowitz, M. & Stegun, I. A. (1964). *Handbook of mathematical functions*. Washington DC: National Bureau of Standards.
- Aynbinder, A. B. & Kamershtein, A. G. (1982). *Raschet magistral'nykh truboprovodov na prochnost' i ustoychivost'* (Calculation of strength and stability of transmission pipelines). Moscow: Nedra.
- Baldry, J. A. S. (1973). *The buckling of axially loaded buried pipelines*. MSc dissertation, Cambridge University.
- Barefoot, A. J. (1997). *Upheaval buckling of subsea pipelines*. MEng dissertation, Cambridge University.
- Barker, H. R. (1998). *Physical modelling of construction processes in the mini-drum centrifuge*. PhD dissertation, Cambridge University.
- Baumgard, A. J. (2000). *Monotonic and cyclic soil responses to upheaval buckling in offshore buried pipelines*. PhD dissertation, Cambridge University.
- Cuckson, J. (1977). *Shear zones and progressive failure in over-consolidated clay*. PhD dissertation, Cambridge University.
- Dempsey, J. P., Palmer, A. C. & Sodhi, D. S. (2001). High pressure zone formation during compressive ice failure. *Engineering Fracture Mechanics* **68**, 1961–1974.
- Fisher, R., Powell, T., Palmer, A. C. & Baumgard, A. J. (2002). Full scale modelling of subsea pipeline uplift. *Proceedings of the physical modelling in geotechnics conference*, St John's, Newfoundland.
- Garnier, J. (2002). Size effect in shear interfaces. *Proceedings of the workshop on constitutive and centrifuge modelling: two extremes*, Monte Verita, Switzerland, pp. 335–346.
- Mokni, M. & Desrues, J. (1998). Strain localization measurements in undrained plane-strain biaxial tests on Hoston RF sand. *Mechanics of Cohesive-Frictional Materials* **4**, 419–441.

- Ng, C. W. W. & Springman, S. M. (1994). Uplift resistance of buried pipelines in granular materials. *Proceedings Centrifuge 94*, pp. 753–758. Rotterdam: Balkema.
- Nielsen, N.-J. R., Lyngberg, B. & Pedersen, P. T. (1990). Upheaval buckling failures of insulated flowlines: a case story. *Proc. 22nd Offshore Technol. Conf., Houston* **4**, 581–592.
- Palmer, A. C. (1991). Centrifuge modelling of ice and brittle materials. *Can. Geotech. J.* **28**, 896–898.
- Palmer, A. C. & Baldry, J. A. S. (1974). Lateral buckling of axially compressed pipelines. *J. Pet. Technol.* **26**, 1283–1284.
- Palmer, A. C. & Johnston, I. E. (2001). Ice velocity effects and scaling. *Proceedings of the IUTAM symposium on scaling laws in ice mechanics and ice dynamics*, Fairbanks, AK, June 2000, pp. 115–126.
- Palmer, A. C. & Rice, J. R. (1973). The growth of slip surfaces in the progressive failure of overconsolidated clay. *Proc. R. Soc. London Ser. A* **332**, 527–548.
- Palmer, A. C. & Sanderson, T. J. O. (1991). Fractal crushing of ice and brittle solids, *Proc. R. Soc. London Ser. A* **433**, 469–477.
- Palmer, A. C., Ellinas, C. P., Richards, D. M. & Guijt, T. J. (1990). Design of submarine pipelines against upheaval buckling. *Proc. 22nd Offshore Technol. Conf., Houston* **2**, 551–560.
- Palmer, A. C., Carr, M., Maltby, T., McShane, B. & Ingram, J. (1994). Upheaval buckling: what do we know, and what don't we know? *Proceedings of the offshore pipeline technology seminar*, Oslo.
- Petley, D. J. (1966). *The shear strength of soils at large strains*. PhD dissertation, University of London.
- Roger, V., Desrues, J. & Viggiani, G. (1998). Experiments on strain localisation in dense sand under isochoric conditions. *Proc. 4th Int. Workshop on Localisation and Bifurcation Theory for Soils and Rocks, Gifu*, 239–248.
- Sanderson, T. J. O. (1988). *Ice mechanics: Risks to offshore structures*. London: Graham & Trotman.
- Sture, S., Alquasabi, A. & Ayari, M. (1999). Fracture and size effect characters of cemented sand. *International Journal of Fracture* **95**, 405–433.
- Van Mier, J. G. M. (1997). *Fracture processes of concrete: Assessment of material parameters for fracture models*. Boca Raton, FL: CRC Press.
- Van Mier, J. G. M. (2001). Microstructural effects on fracture scaling in concrete, rock and ice. *Proceedings of the IUTAM symposium on scaling laws in ice mechanics and ice dynamics*, Fairbanks, AK, June 2000, pp. 171–182.
- White, D. J., Barefoot, A. J. & Bolton, M. D. (2000). *Centrifuge modelling of upheaval buckling in sand*, Technical report CUED/D-SOILS/TR314. University of Cambridge.